JOURNAL OF MATERIALS SCIENCE **35** (2000) 4449 – 4457

New features of the low temperature ductile shear failure observed in bulk amorphous alloys

V. Z. BENGUS, E. D. TABACHNIKOVA
B.Verkin Institute for Low Temperature Physics & Engineering of National Academy of Sciences of Ukraine, 47, Lenin's Ave. Kharkov, 310164, Ukraine
E-mail: bengus@ilt.kharkov.ua

J. MIŠKUF, K. CSACH, V. OCELÍK
Institute of Experimental Physics of Slovak Academy of Sciences, 47, Watson Str., 043 53 Košice, Slovakia
E-mail: miskuf@saske.sk

W. L. JOHNSON
W.M. Keck Laboratory of Engineering Materials, 138-78, California Institute of Technology, Pasadena, California 91125, USA

V. V. MOLOKANOV
A. Baikov Institute of Metallurgy of Russia Academy of Sciences, 49 Leninski Ave., Moscow, 117, GSP, Russia

Fractographic studies of ductile shear failure under the uniaxial compression for rod–like samples of the $Zr_{41.2}Ti_{13.8}Ni_{10}Cu_{12.5}Be_{22.5}$ and $Cu_{50}Zr_{35}Ti_8Hf_5Ni_2$ bulk amorphous alloys at temperatures 300 and 77 K are presented. The mechanisms of shear deformation and failure appeared to have characteristics in common with other amorphous alloys prepared in the form of thin ribbons. However, there were a number of new fractographic features observed due to the bulk character of the samples and to the large supercooled liquid region of these alloys.

1. Introduction

The physical processes of catastrophic shear and ductile shear failure in amorphous alloys have been studied for many years, but mainly on thin ribbons [1–3]. In this case, the failure usually takes place under the conditions of antiplane strain by the movement of a shear crack (of type III according to the generally accepted classification [4]). Therefore, established features of the failure and meniscus instability on the failure surfaces are related mainly to cracks of type III. The type II cracks (oriented along the zero elongation direction – "53° – failure mode" [5]) are also observed in the failure of ribbons. In the course of failure under tension, these cracks are transformed into type I with the occurrence of some differences in failure regularities [6].

It is known that the meniscus instability [7] in the volume of the strongly heated catastrophic shear band occurs at the final stages of the ductile shear failure of amorphous alloys. Due to local adiabatic deformation heating [2, 3, 8], there is a rapid increase in the local temperature of material inside the catastrophic shear band that leads to this materials behaving in a superplastic [9] manner with a small viscosity ('liquid-like' [2]). The meniscus instability during the rupture of this 'liquid-like' layer leads to the formation of a 'vein pattern' on the failure surfaces. An analysis of this vein pattern has lead to the discovery of some important features of the amorphous metallic alloys behavior during the failure as follows:

– the local temperature of the material in the 'liquid-like' layer approaches the melting point [3, 10];
– being liquid-like, the material in the hot layer is nevertheless solid [3];
– the material in the 'liquid-like' layer exhibits superplasticity (phenomenologically similar to the liquid with a small viscosity) [9, 11];
– there appears to be local melting of material during the rupture as indicated by solidified drops of the melt on the fracture surfaces [3, 10, 11].

These features were discovered mainly when failure proceeded by the spreading of a type–III crack through the ribbon of the amorphous alloys.

The shear failure process and the meniscus instability in new generation amorphous alloys with a large interval of vitrification – bulk amorphous alloys [12–14] show some new features. Vein patterns have also been observed in the fracture surface of bulk amorphous alloy that have loaded in compression. From this it was concluded that adiabatic heating [2] was the only process that determines the existence of the 'liquid-like' layer [15, 16].

Since the ductile shear failure of bulk amorphous alloys rods under compression is by a type II crack (which is transformed to the type I at the final stage of the failure), one may expect that the set of features that were discovered earlier for failure by the spread of the type–III crack could be increased. For instance, the soft material of the 'liquid–like' layer should be (under compression) squeezed out from the catastrophic shear band and this may give rise to the new features observed in the fractographic pictures. However, a detailed analysis of the 'vein patterns' in the bulk amorphous alloys and their comparison with those of thin ribbons of usual amorphous alloys has not been carried–out up to the present.

Further observations and analysis of the vein patterns on the shear failure surfaces formed during compression loading of bulk amorphous alloys and a comparison with those formed during tensile tests of typical* amorphous alloys ribbons are the subjects of this paper.

2. Materials and methods

Mechanical properties and vein patterns at the shear failure surfaces where studied for bulk amorphous metallic alloys $Zr_{41.2}Ti_{13.8}Ni_{10}Cu_{12.5}Be_{22.5}$ (prepared as a drop–like ingot with 40 mm in diameter on a cooled substrate [14]) and $Cu_{50}Zr_{35}Ti_8Hf_5Ni_2$ (prepared as 6 mm rods by casting to a copper mould [13]).

The failure stress for uniaxial compression of the cylindrical (3 mm in diameter $\times$ 9 mm) or prismatic ($3 \times 3 \times 9$ mm) samples were measured with a tensile/compression testing machine (with a relative high rigidity of 10 kN/mm) at a compression rate of 0.15 mm/min at 300 and 77 K. Fractography observations were made using a TESLA BS300 Scanning Electron Microscope (SEM).

3. Experimental results

3.1. Mechanical properties

The failure stress (σ_f) of the $Zr_{41.2}Ti_{13.8}Ni_{10}Cu_{12.5}Be_{22.5}$ amorphous alloy under compression at temperature 300 K was 1.75 ± 0.25 GPa. As the scatter of the measured failure stress was relatively large, it can be considered to be similar to 1.91 ± 0.03 GPa measured in [17] or to 1.8 ± 0.023 GPa measured in [18]. At a temperature of 77 K, the σ_f was 1.35 ± 0.35 GPa.

The plane of the failure surface was close to the plane of the maximum shear stresses, i.e. 45 degrees to the compression axis (Fig. 1a). Catastrophic plastic shear preceeded failure and typical vein patterns were formed at the fracture surfaces (Fig. 2a). At 77 K the fracture surface was not as simple. In addition to the ductile shear failure mode, the normal rupture mode with the fracture surface perpendicular to the sample axis was realized. Therefore, 'chevron pattern' [1, 19] is present on some areas of the fracture surface (Fig. 2b) formed during the final stages of the failure after the loss of stability by the sheared sample under the uniaxial compression.

* By this we mean amorphous alloys with a small interval of vitrification which are usually prepared in the form of thin ribbons.

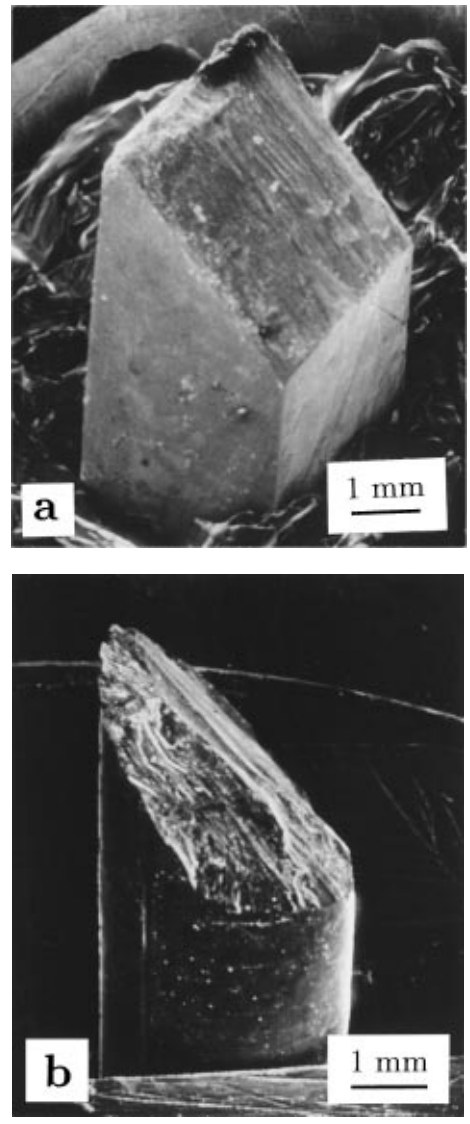

Figure 1 SEM macrofractographs of the shear failure surfaces of the bulk amorphous alloys fractured by uniaxial compression at 300 K: a) $Zr_{41.2}Ti_{13.8}Ni_{10}Cu_{12.5}Be_{22.5}$ prismatic sample; b) $Cu_{50}Zr_{35}Ti_8Hf_5Ni_2$ cylindrical sample.

The σ_f of the $Cu_{50}Zr_{35}Ti_8Hf_5Ni_2$ amorphous alloy under compression at 300 K has already been reported [15] to be 1.27 ± 0.06 GPa. The fracture surface was also inclined approximately 45 degrees to the compression axis (Fig. 1b) and example of the vein patterns observed is shown in Fig. 3.

3.2. Fractographic observations

SEM observations of the ductile shear failure surfaces of the bulk amorphous alloys show features that are unique of bulk amorphous alloys and are not typical for first generation amorphous alloys. These features are:

a) A generally anisotropic (elongated in the shear direction) and striated vein pattern (Fig. 4a–c): there are sharply outlined strips of the surface covered by veins (average width of these strips is of the order of 10 μm) alternating with the narrower strips that are usually often free of veins;

b) Near periodic nets of cell–like configurations of veins within the before mentioned strips (Figs 5, 2a, 3);

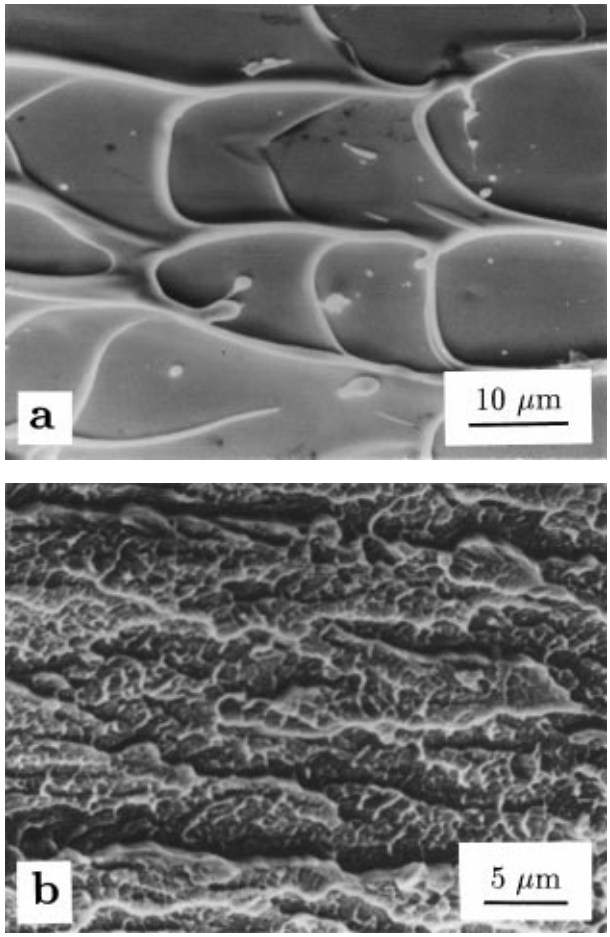

Figure 2 Typical morphologies on fracture surfaces of the $Zr_{41.2}Ti_{13.8}Ni_{10}Cu_{12.5}Be_{22.5}$ amorphous alloy: a) "vein pattern" morphology formed by meniscus instability at 300 K. b) "chevron pattern" morphology formed at 77 K.

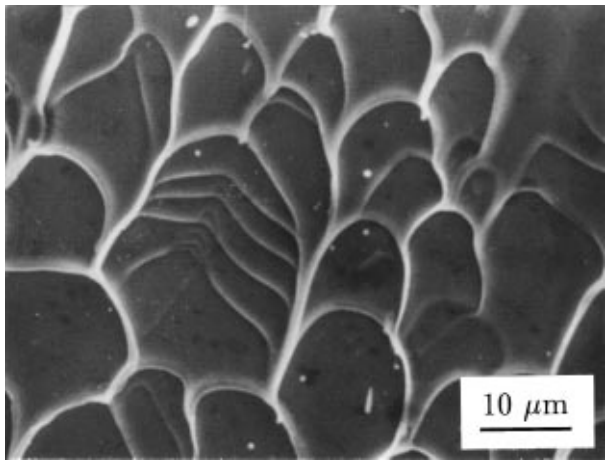

Figure 3 Vein pattern morphology on fracture surface of $Cu_{50}Zr_{35}Ti_8Hf_5Ni_2$ amorphous alloy failed at 300 K.

c) Many protruding veins that have fallen over and overlapped the protruding veins formed previously together with many spheroidal drops (Fig. 6a–c);

d) Wide, flat and elongated veins extending along the shear surface from the edge of the shear step of the sample surface (Fig. 7a, b). In the amorphous alloy ribbons, this part (labelled as part A in the terminology of [19]) of the shear surface is usually smooth and free of veins [20] (Fig. 8);

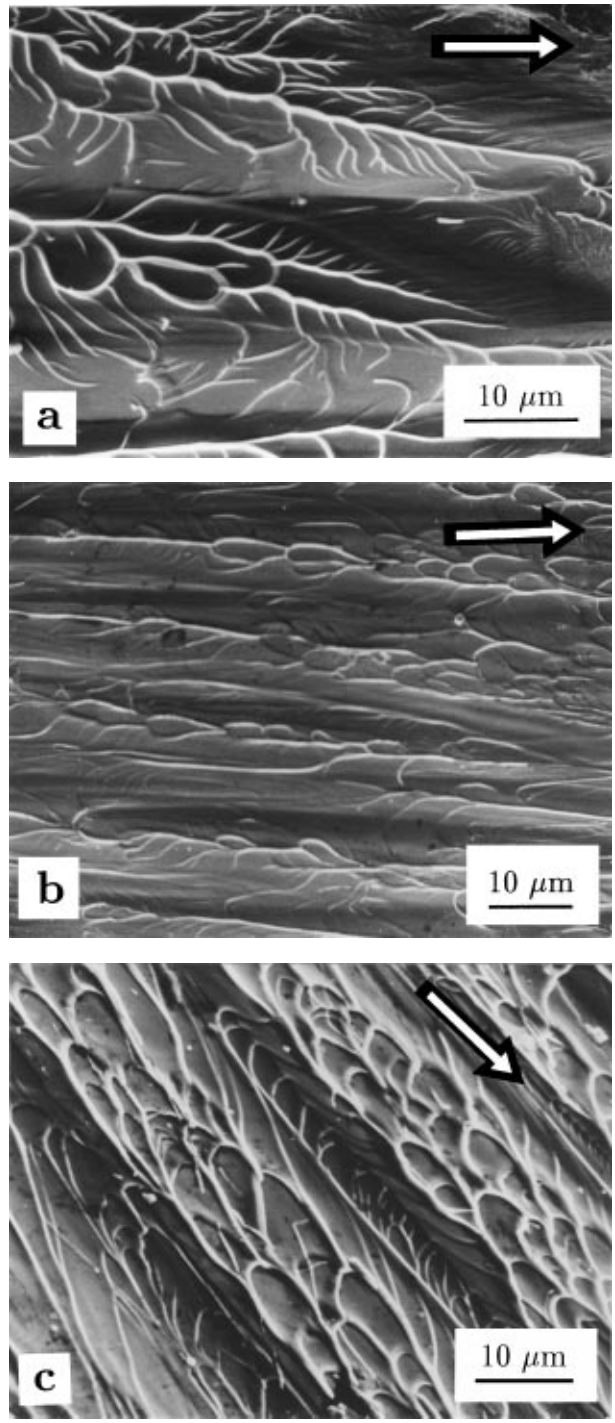

Figure 4 Anisotropic manifestations of the vein pattern morphology in the macroscopic shear direction (indicated by arrows) in: a) $Zr_{41.2}Ti_{13.8}Ni_{10}Cu_{12.5}Be_{22.5}$ alloy at 77 K; b) $Zr_{41.2}Ti_{13.8}Ni_{10}Cu_{12.5}Be_{22.5}$ alloy at 300 K; c) $Cu_{50}Zr_{35}Ti_8Hf_5Ni_2$ alloy at 300 K.

e) The veins are thicker than that observed in usual amorphous alloys (Figs 2a, 3). It seems that these veins have a profile that is more circular than triangular, where the latter is typical cross-sectional of veins in usual amorphous alloys [21].

A schematic sketch of a typical shear fracture surface formed after the compression test of bulk amorphous alloys is shown in Fig. 9. Points a) and b) are observed in the region B. Point c) is observed in the regions B and C. Point d) is observed in the region A.

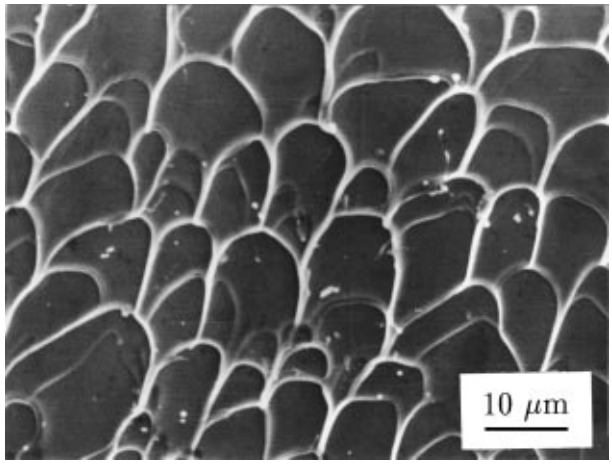

Figure 5 The almost periodical cell structure of veins formed on the $Cu_{50}Zr_{35}Ti_8Hf_5Ni_2$ alloy fracture surface.

4. Discussion

4.1. Non–planar surface of glide

Non–planar surface of glide, which is observed after the low temperature ductile shear failure of the $Cu_{50}Zr_{35}Ti_8Hf_5Ni_2$ and $Zr_{41.2}Ti_{13.8}Ni_{10}Cu_{12.5}Be_{22.5}$ bulk amorphous alloys, is a typical phenomenon (see Fig. 4a for example). The catastrophic glide surface consisted of ridges and valleys oriented approximately parallel to the shear direction. Veins were arranged on the failure surface in two different modes:

– As strips of a cell–like network on the ridges of the fracture surface, similar to the case of ribbons. However, the cell-like character of the vein pattern was much more complicated than that of the ribbon fracture case. Such an arrangement forms an anisotropic and strip–like character of the vein pattern in bulk amorphous alloys (Fig. 4a–c) because strips which are free of veins are formed along the valleys. This arrangement of veins was typical for samples deformed at 300 K;

– Almost independently on relief of fracture surface (Fig. 10). Such a pattern is very different from that observed in amorphous alloys ribbons where the veins were usually formed on the ridges of the failure surface and valleys were free of veins (Fig. 8). This arrangement of the veins was typical for samples deformed at 77 K.

The non–planar character of the glide surface is probably caused by macroscopic defects on the sample's surface. The catastrophic slip can be considered to be initiated by heterogeneous surface nucleation at such defects [22]. The role of such macroscopic defects in amorphous alloys had been demonstrated by the correlation of the Weibull's statistics [23] to the distribution of failure stresses of amorphous alloys [24–27]. Therefore, the width of the strips must correspond to the linear dimensions of surface defects at which heterogeneous nucleation of the catastrophic slip occurs. Such a correlation was easily observed in this study.

According to Bakai [28], slip in amorphous alloys spreads preferentially along intercluster boundaries. Therefore, the profile of macroscopic glide surface should be predetermined by an incidental configuration of the slip initiated at surface defects. The glide surface was formed by the areas of intercluster boundaries surfaces oriented parallel to the shear direction and to the plane of the maximum shear stresses.

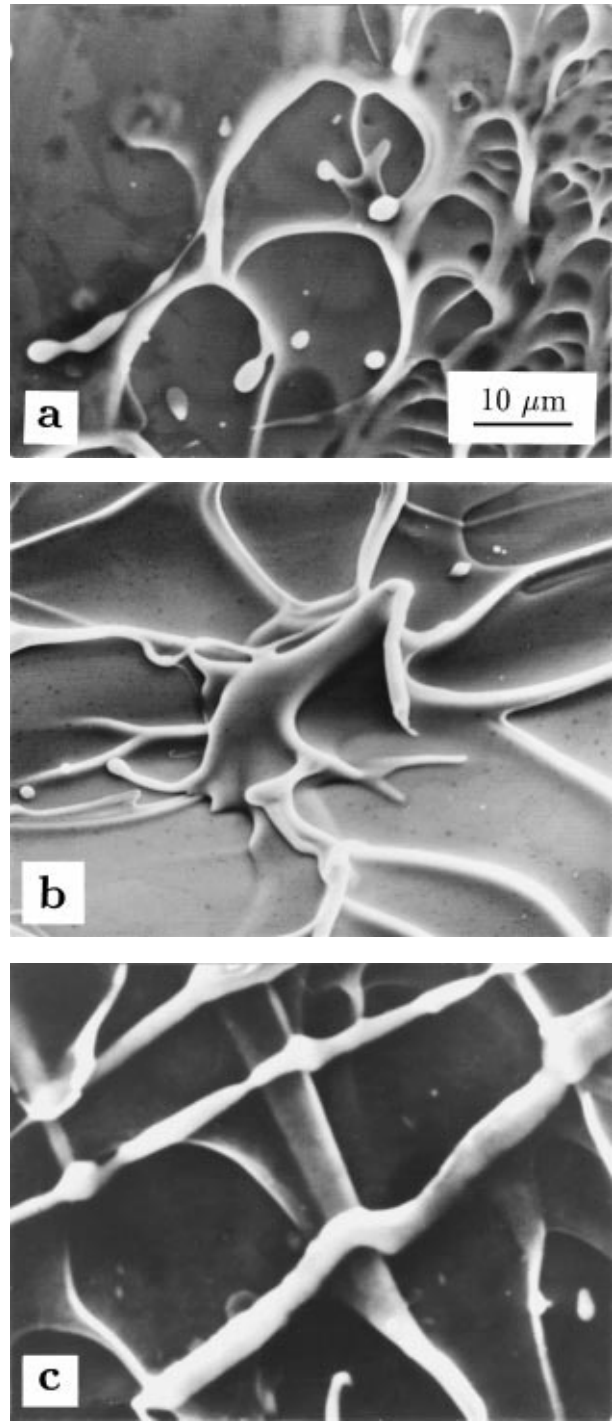

Figure 6 Fractographic features formed by the relicts of protruding veins on fracture surfaces of both $Cu_{50}Zr_{35}Ti_8Hf_5Ni_2$ (a, c) and $Zr_{41.2}Ti_{13.8}Ni_{10}Cu_{12.5}Be_{22.5}$ (b) alloy failed at 300 K.

4.2. Homogeneous nucleation of meniscus instability in bulk amorphous alloys

During the low temperature ductile shear failure of amorphous alloy ribbons, the nucleation of meniscus instability takes place heterogeneously at the surfaces of the ribbon (i), or at voids or inclusions in the sample (ii). This instability nucleates at the point of intersection of the ribbon's surface with the shear crack front and

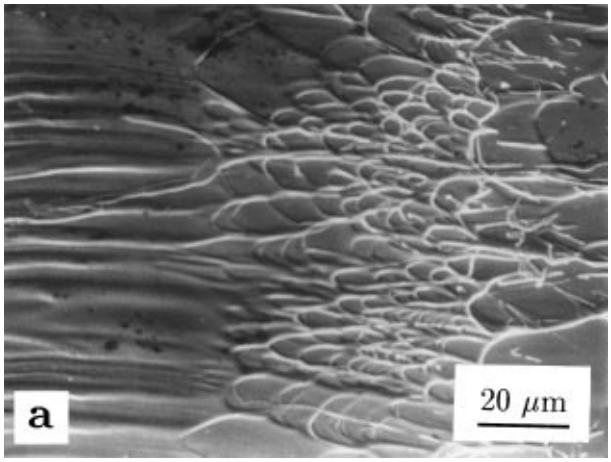

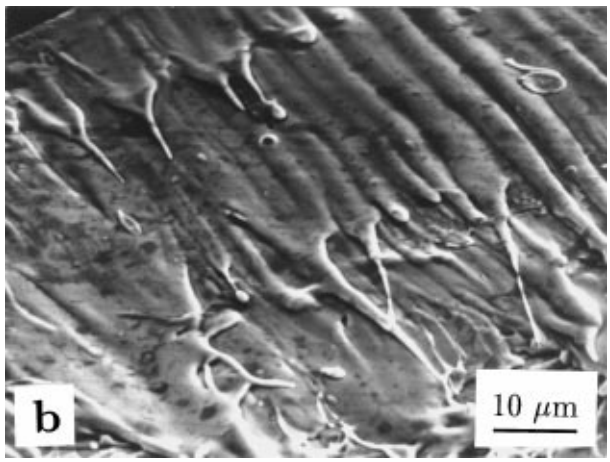

Figure 7 The shear fracture surface near the edge of a shear step on: a) $Zr_{41.2}Ti_{13.8}Ni_{10}Cu_{12.5}Be_{22.5}$; b) $Cu_{50}Zr_{35}Ti_8Hf_5Ni_2$ amorphous samples both failed at 300 K.

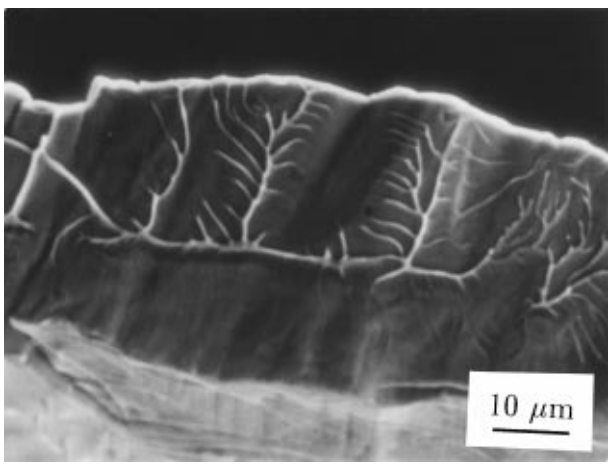

Figure 8 "Smooth" and "vein pattern" morphologies observed in 30 μm thick $Ni_{78}Si_8B_{14}$ amorphous ribbon failed at uniaxial tension at 4.2 K.

spreads successively along the failure surface together with the spreading of the type III crack.

The heterogeneous character of meniscus instability nucleation at the surface of amorphous ribbon is well illustrated by the dependence of distance d between veins on the ribbon's surfaces. This distance was different for the veins initiated at dull and shining surface of a ribbon. This difference is shown in Fig. 11 where histograms of statistical distribution of distance d measured from the sample shown in Fig. 12 are presented.

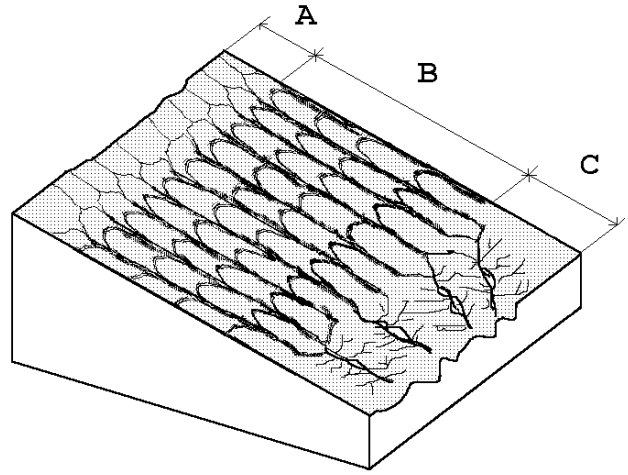

Figure 9 Schematic sketch of a typical shear failure surface formed during the compression test of bulk amorphous sample. The character of three typical regions are described in the text.

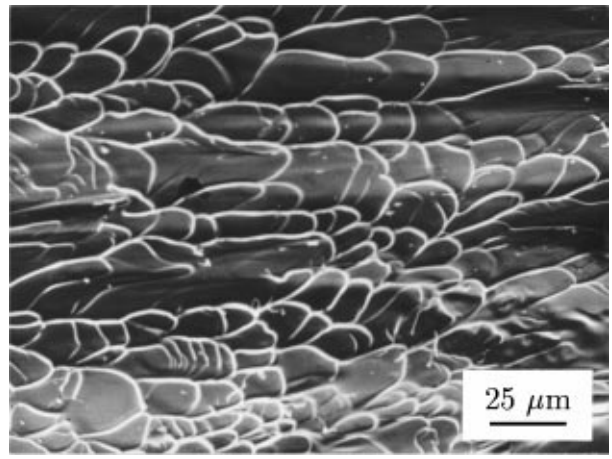

Figure 10 The cellular "vein pattern" morphology in the $Zr_{41.2}Ti_{13.8}Ni_{10}Cu_{12.5}Be_{22.5}$ bulk amorphous alloy failed at 300 K.

The average value of d measured near a dull surface is higher than that for the shining surface.

The non-surface nucleation of meniscus instability is rarely observed (Fig. 13). This nucleation usually takes place during the failure by the spread of the type II crack (the 'oblique' mode of the failure [1, 5] along the zero elongation direction). The internal nucleation is often connected with voids and inclusions in amorphous alloys ribbons [10]. To the authors knowledge, the homogeneous nucleation of meniscus instability has never been observed in amorphous alloys ribbons.

Another event observed in the rods of bulk amorphous alloys failed under compression was the transformation of the type II crack into a type I crack at the loss of stability in the strained sample at large deformations. In addition to the vein patterns (see Fig. 4a) formed by the heterogeneous nucleation of the meniscus instability, many cell–like veins like that observed in the vein pattern strips of bulk amorphous alloys were observed. This indicates that the nucleation of the meniscus instability can also take place along the failure surface simultaneously at many points (at the centers of cells) behind the front of opening crack of the type I. The almost equal dimensions of cells in Fig. 5 indicate that

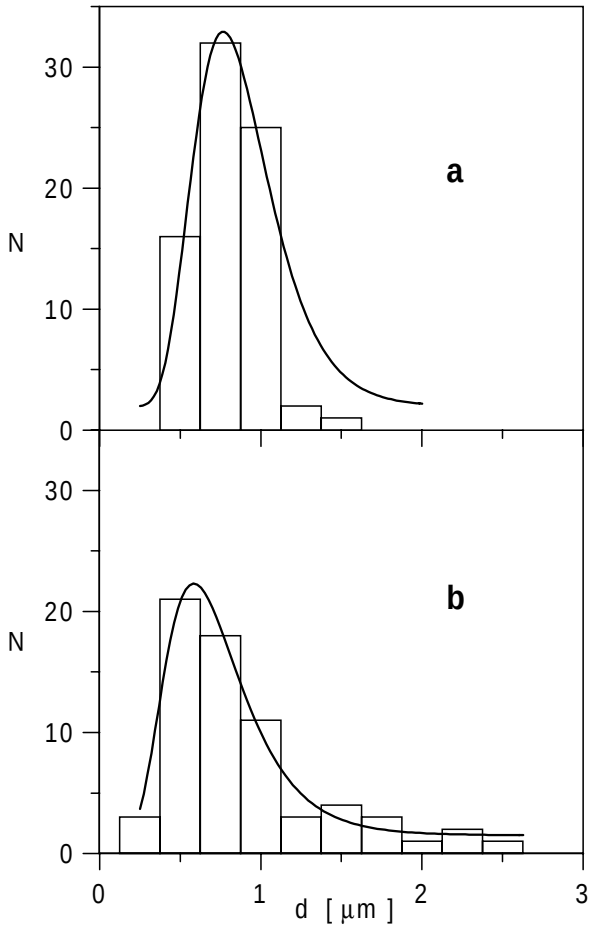

Figure 11 Statistical distributions of distances d between the veins measured near the shinning (a) and dull (b) side of amorphous ribbon shown on Fig. 12. The mean values of d are 0.67 ± 0.21 μm near the shinning and 0.77 ± 0.48 μm near the dull side of the ribbon.

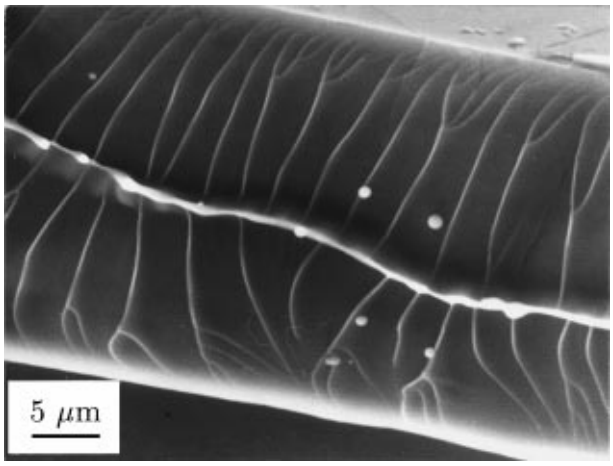

Figure 12 A "vein pattern" morphology with a main vein at the centre of ribbon, formed after the shear that was parallel to the ribbon surface, when the meniscus instability is initiated from both sides of shear band at the same time. A $Fe_{84}B_{16}$ amorphous ribbon, failed by tensile stress at 300 K.

similar conditions were present at many of the nucleation points. The simultaneous nucleation events must substantially increase the contribution of the work of plastic deformation to the apparent surface energy γ_f (which includes the work of plastic deformation) of the material compared with the heterogeneous nucleation

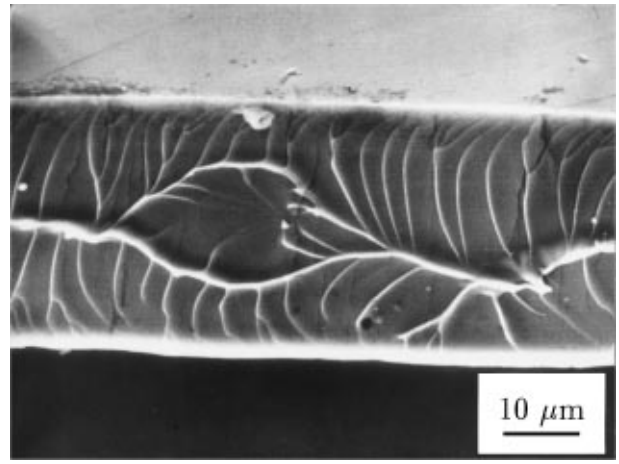

Figure 13 Non-surface initiation of meniscus instability, rarely observed on amorphous ribbons. $Fe_{84}B_{16}$ amorphous ribbon, failed by tensile strain at 300 K with the strain rate of $2 \times 10^{-2} s^{-1}$.

of meniscus instability in amorphous ribbons. To see this, one can estimate the apparent surface energy, γ_f, of the material during the cell–like veins pattern formation and compare it with a typical vein pattern observed in amorphous alloys ribbons. This can be done with the formula

$$\gamma_f = (12\pi^2 1.2\sqrt{3})^{-1} \times \frac{\sigma_f}{N}, \qquad (1)$$

from the theory of Argon and Salama [29] for the meniscus instability during the ductile shear failure of amorphous alloys using experimental measurements of linear density N of veins and of the failure stress σ_f. Values for N are taken to be the inverse of cells diameters. The results are shown in the Table I.

It can be seen that γ_f in the bulk amorphous alloys studied here are several times larger than the γ_f estimated for a typical ductile amorphous alloy ribbon (for example $Ni_{78}Si_8B_{14}$ [20]) where heterogeneous nucleation of meniscus instability evidently takes place. The almost two orders of magnitude difference in γ_f above that for typical surface energies of solids (of the order of 1 J/m^2 [30]) is explained by the work of plastic deformation of material during the vein-pattern formation. The larger work of plastic deformation during the vein-pattern formation in bulk amorphous alloys than in amorphous ribbons is therefore observed.

The observed networks of cells (Figs 2a, 3, 5) closely resemble the morphology of coalescing microvoids typical of the ductile failure of structural alloys under a shear strain (Chapter 5 of [4]). A schematic sketch of arising of such pattern (analogous to Fig. 5.10 in [4]) is shown in Fig. 14. This figure shows multiple homogeneous nucleation of the meniscus instability inside samples of bulk amorphous alloys during rupture along the surface of the preceding catastrophic shear (B region in Fig. 9).

A supposition about the heterogeneous nucleation of meniscus instability at microscopic inclusions (below the resolution of the SEM) can be rejected since the bulk amorphous alloys were prepared from very pure materials and oxides in the $Zr_{41.2}Ti_{13.8}Ni_{10}Cu_{12.5}Be_{22.5}$

TABLE I Estimation of the material apparent surface energy γ_f during the meniscus instability on the low temperature ductile shear failure surfaces of the $Cu_{50}Zr_{35}Ti_8Hf_5Ni_2$ and $Zr_{41.2}Ti_{13.8}Ni_{10}Cu_{12.5}Be_{22.5}$ bulk amorphous alloys

	σ_f, GPa		N, 10^4 m^{-1}		γ_f, J/m^2	
Alloy composition	300 K	77 K	300 K	77 K	300 K	77 K
$Zr_{41.2}Ti_{13.8}Ni_{10}Cu_{12.5}Be_{22.5}$	1.75 ± 0.25	1.35 ± 0.35	7.2	5.5	~97	~98
$Cu_{50}Zr_{35}Ti_8Hf_5Ni_2$	1.27 ± 0.06	–	8.3	–	~61	–
$Ni_{78}Si_8B_{14}$ [20]	2.25	2.65	32	38	~28	~28

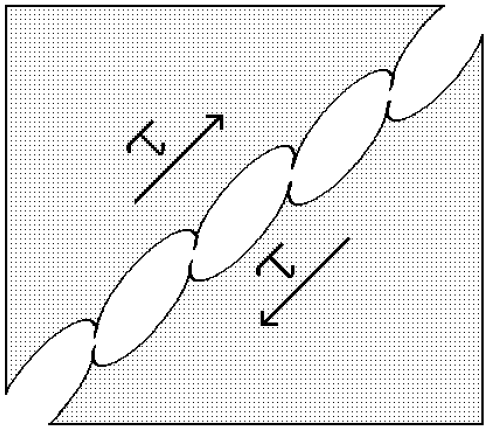

Figure 14 A schematic sketch of cells net arising by the coalescence of microvoids under shear strain.

amorphous alloy are not present [31]. Therefore, the presence a multitude of small inclusions necessary for the cell–like vein pattern formation through the heterogeneous nucleation is considered unlikely.

At the same time, heterogeneous nucleation of the meniscus instability is often observed in addition to the homogeneous nucleation at certain regions of the failure surface. This can be seen in Fig. 4a.

4.3. Evidence of the local hot state of the material on the shear failure surfaces

Previous experimental measurements of the integral heating of amorphous alloy ribbons under the ductile shear failure at 0.5 K [3] enable an estimate to made of the temperature increase in the catastrophic shear band due to the local deformation. These estimates indicate that temperatures approaching the melting point can be achieved. Previous fractographic observations [10, 11] show evidence of a liquid phase present at the last stage of the shear failure (during the rupture) by the presence of spheroidal drops that had probably formed during the failure of protruding veins.

Vein patterns in the bulk amorphous alloys also seem to indicate a pre-melting state of the material at the shear failure surfaces. There were spheroidal drops and peaces of the protruding 'veins' that have been flung during the rupture of the failure surfaces and then fallen back onto the fracture surfaces. This process appears to occur more than once (two to three times) and results in overlapping like that seen in the Fig. 6c. Such behavior may be a consequence of the several orders of magnitude larger interval of vitrification of bulk amorphous alloys [31] compared to typical amorphous alloys. Therefore, the pieces of the protruding veins and droplets that are jettisoned from the surface during failure may retain their superplastic state [9] during their flight and upon falling upon the failure surfaces, like that shown in the Fig. 6c.

To verify such a notion, let us estimate the time t_c that a drop of the $Zr_{41.2}Ti_{13.8}Ni_{10}Cu_{12.5}Be_{22.5}$ amorphous alloy flying through the air needs in order cool from the pre–melting state (below solidus) down to T_g. For the simplicity, let us consider a 1 μm spheroidal drop with the initial temperature T_0 flying with a velocity of 1 m/s in air. Then, according to [32] (Ch. XIII, formula 9.22), an estimation can be made of t_c from

$$t_c \approx \frac{T_0 - T_g}{T_0} \times \frac{a}{kh\kappa}, \qquad (2)$$

where a is a radius of the spheroidal drop, $k = 4\pi a^3 \rho c / M_d c_d$, $h = H/K$, κ is the coefficient of heat diffusion of the air, K is its thermal conductivity, H is the coefficient of surface heat transfer, ρ is air density, c is the specific heat of air, M_d and c_d are the mass and specific heat of the drop correspondingly. From $T_0 = 925$ K, $T_g = 625$ K [31], $a = 0.5$ μm, $M_d = 4.6 \times 10^{-16}$ kg, $c_d \simeq 25$ J/K·mol, $\rho = 1.2$ kg/m^3, $c = 1005$ J/kg·K, $\kappa = 2.16 \times 10^{-5}$ m^2/s, $K = 2.6 \times 10^{-2}$ J/m·s·K, $H \simeq 3.34 \times 10^3$ J/m^2·s·K, one can find $t_c \sim 40$ μs. This time interval is one order of magnitude larger than the time measured for failure [3]. Therefore, the pieces of the protruding veins falling upon the failure surfaces are probably at a high enough temperature to be superplastic, thus enabling them to wrap around the prior formed veins on the failure surfaces. This can be considered additional evidence that a hot local state of material existed during the ductile shear failure of bulk amorphous alloys.

Further evidence of a high temperature state at the shear fracture surfaces is the observation mentioned in 3.2d. The wide, flat and elongated veins extending along the shear surface from the edge of the shear step at the surface of the sample may arise from the squeezing–out of soft (superplastic) material originally present in the catastrophic shear band following the shear crack due to sample being under compression. In amorphous alloy ribbons, this part of the shear surface is usually smooth and free of any veins because under the tension there is no such squeezing–out action.

The more equilibrium form of the veins in bulk amorphous alloys (point 3.2 e) is probably observed due to the larger duration in the soft superplastic state, which is enough to achieve this form under the action of surface tension.

4.4. Peculiarities of the low temperature ductile failure of the $Zr_{41.2}Ti_{13.8}Ni_{10}Cu_{12.5}Be_{22.5}$ bulk amorphous alloy

The mechanical properties of bulk amorphous alloys below the room temperature have never been reported in literature before. The small decrease in σ_f for the $Zr_{41.2}Ti_{13.8}Ni_{10}Cu_{12.5}Be_{22.5}$ alloy observed with cooling from 300 to 77 K and the presence of chevron patterns on the low temperature fracture surface indicate an apparent decrease in the plasticity. This is usually caused by premature rupture (before attaining the yield stress) owing to a decohesion at the surface of occasional crystalline inclusions [20] which may be available in amorphous alloys [10]. Moreover, crystalline particles may be present in this alloy [18, 33].

The observed decrease in σ_f with cooling is within the limits of the scatter in experimental data and it is doubtful that there is a real decrease of plasticity in the $Zr_{41.2}Ti_{13.8}Ni_{10}Cu_{12.5}Be_{22.5}$ bulk amorphous alloy at 77 K. Indeed, comparison of the estimated γ_f for this alloy at 300 and 77 K on the basis of the Argon and Salama theory [29] (see Table I), one can conclude that the contribution of the work of plastic deformation is not decreased when cooled to 77 K. This can be considered an indirect indication of retaining the plasticity of the $Zr_{41.2}Ti_{13.8}Ni_{10}Cu_{12.5}Be_{22.5}$ amorphous alloy at 77 K. Real knowledge of the ductility of this alloy at low temperatures requires further direct experimental study.

5. Concluding remarks

Fractographic observations of surfaces of the ductile shear failure under compression of the $Zr_{41.2}Ti_{13.8}Ni_{10}Cu_{12.5}Be_{22.5}$ and $Cu_{50}Zr_{35}Ti_8Hf_5Ni_2$ bulk amorphous metallic alloys have revealed features never been observed in amorphous alloys ribbons before as follows:

1. Striated vein patterns (extended along the shear direction) containing periodical nets of the cell–like configurations of veins. The homogeneous nucleation of the meniscus instability is considered as the most probable cause for these configurations. Such nucleation is accompanied by a larger work of plastic deformation than for heterogeneous nucleation that is typical of common amorphous alloys ribbons.

2. Wide, flat, elongated, non–branching veins extended along the shear surface from the edge of the shear step near the surface of a sample. These veins appear to be formed by the squeezing–out of a soft-hot material from the catastrophic shear band that is under compression of the sample.

3. Pieces of the protruding veins lying on the failure surface and that are overlapped (twice and three times) with veins that were formed earlier in the failure. This phenomenon is considered to be a consequence of conserving the superplastic state of veins during times even larger than the failure time due to more than one order larger interval of vitrification of bulk alloys than in common amorphous alloys ribbons.

References

1. L. A. DAVIS, in "Metallic Glasses," edited by J. J. Gilman and H. J. Leamy (ASM, Metals Park, OH, 1978) p. 190.
2. H. Y. LEAMY, H. S. CHEN and T. T. WANG, *Metallurgical Transactions* **3** (1972) 699.
3. V. Z. BENGUS, E. D. TABACHNIKOVA, S. E. SHUMILIN, Y. I. GOLOVIN, M. V. MAKAROV, A. A. SHIBKOV, J. MIŠKUF, K. CSACH and V. OCELÍK, *Int. J. of Rapid Solidification* **8** (1993) 21.
4. R. W. HERTZBERG, "Deformation and Fracture Mechanics of Engineering Materials" (John Wiley & Sons, N.Y., 1983).
5. V. Z. BENGUS, P. DIKO, K. CSACH, J. MIŠKUF, V. OCELÍK, E. B. KOROLKOVA, E. D. TABACHNIKOVA and P. DUHAJ, *J. Mater. Sci.* **25** (1990) 1598.
6. V. OCELÍK, V. Z. BENGUS, E. B. KOROLKOVA, K. CSACH, J. MIŠKUF and P. DUHAJ, *ibid.* **26** (1991) 6699.
7. A. S. ARGON, "Glass Science and Technology" Vol. 5 (Academic Press, New York, 1980) P. 5, 79.
8. H. A. BRUCK, A. J. ROSAKIS and W. L. JOHNSON, *J. of Materials Research* **11** (1996) 503.
9. V. BENGUS, E. TABACHNIKOVA, K. CSACH, J. MIŠKUF and V. OCELÍK, *Scripta Metallurgica et Materialia* **35** (1996) 781.
10. V. Z. BENGUS, in "Non linear phenomena in materials science II" edited by G. Martin and L. Kubin (Trans Tech Publications, Zurich 1992) *Solid State Phenomena* **23/24** (1992) 347.
11. V. BENGUS and V. OCELÍK, *Journal de Physique IV* **7 C3** (1997) C3-939.
12. A. INOUE, T. ZHANG and T. MASUMOTO, *Mater. Trans. JIM* **31** (1990) 177.
13. V. V. MOLOKANOV, T. N. MIKHAILOVA and V. N. CHEBOTNIKOV, Abstracts of the II European West-East Symposium on Materials and Processes (MATTEX-91) May 1991, Finland, 68.
14. A. PEKER and W. JOHNSON, *Appl. Phys. Letters* **63** (1993) 2342.
15. E. D. TABACHNIKOVA, V. Z. BENGUS, V. V. MOLOKANOV and T. N. MIKHAILOVA, *Phys. Solid State* **36** (1994) 1280.
16. E. D. TABACHNIKOVA, V. Z. BENGUS and V. V. MOLOKANOV, "Materials Science Forum" Vol. 225–227 Part 1 (Trans Tech Publications, Switzerland, 1996) p. 107.
17. H. A. BRUCK, T. CHRISTMAN, A. J. ROSAKIS and W. L. JOHNSON, *Scripta Metall. Mater.* **30** (1994) 429.
18. P. LOWHAPHANDU and J. J. LEWANDOWSKI, *Scripta Materialia* **38** (1998) 1811.
19. C. A. PAMPILLO, *J. Mater. Sci.* **10** (1975) 1194.
20. V. Z. BENGUS, E. D. TABACHNIKOVA, V. V. HAJKO, JR., P. DIKO, J. MIŠKUF and V. OCELÍK, *Metallofizika* **8**(6, 3) (1986) (in Russian).
21. D. M. KULAWANSA, J. T. DICKINSON, S. C. LANGFORD and Y. WATANABE, *J. Mater. Res.* **8** (1993) 2543.
22. J. C. M. LI, "Metallic Glasses" ASM Seminar 1976 (American Society for Metals, Metals Park, Ohio, 1978) p.224.
23. W. WEIBULL, *J.Appl. Mech.* **18** (1951) 293.
24. M. CALVO, *J. Mater Sci.* **24** (1989) 1801.
25. V. OCELÍK, V. Z. BENGUS, E. B. KOROLKOVA, K. CSACH, J. MIŠKUF and P. DUHAJ, *ibid.* **26** (1991) 6699.
26. V. Z. BENGUS, G. VLASÁK, P. DUHAJ, V. OCELÍK, E. D. TABACHNIKOVA, G. V. BILETCHENKO, E. B. KOROLKOVA, L. D. SON, V. S. TSEPELEV, S. V. ORLOV and V. V. SMIRNOV, "Key Engineering Materials" Vol. 81/83 (Trans Tech Publications, Switzerland, 1993) p. 501.
27. E. D. TABACHNIKOVA, I. P. MANIKA and V. Z. BENGUS, "Key Engineering Materials" Vol. 81–83 (Trans Tech Publications, Switzerland, 1993) p. 135.
28. A. S. BAKAI, in "Topics in Applied Physics 72, Glassy Metals III," edited by H. Beck and H.-J. Günterodt (Springer, Berlin, 1994) 209.
29. A. ARGON and M. SALAMA, *Mater. Sci. Eng.* **23** (1976) 219.

30. in "Tables of Physical Quantities, Reference Book" edited by I. K. Kikoin (Atomizdat, Moscow, 1976) p. 1008 (in Russian).
31. W. L. JOHNSON and A. PEKER, in "Science and Technology of Rapid Solidification and Processing," edited by M. A. Otooni (Kluwer Academic Publishers, Netherlands, 1995) p. 25.
32. H. S. CARSLAW and J. C. JAEGER, "Conduction of Heat in Solids" (Clarendon Press, Oxford, 1959).
33. R. D. CONNER, A. J. ROSAKIS, W. L. JOHNSON and D. M. OWEN, *Scripta Materialia* **37** (1997) 1373.
34. F. SPAEPEN and D. TURNBULL, *Scripta Metallurgica* **8** (1974) 563.
35. F. SPAEPEN, *Acta Met.* **23** (1975) 615.

Received 22 September 1998
and accepted 8 March 2000